Original Research Article

Title: **RNA binding protein Musashi-2 regulates PIWIL1 and TBX1 in mouse spermatogenesis**[1]

Authors and affiliations: Jessie M Sutherland 0000-0001-9672-2371[1,2*], Alexander P Sobinoff[2,3], Barbara A Fraser[2], Kate A Redgrove[2], Nicole A Siddall[4], Peter Koopman[5], Gary R Hime[4], & Eileen A McLaughlin[2, 6]

[1]School of Biomedical Science & Pharmacy, University of Newcastle, Callaghan, 2308 AUS

[2]Priority Research Centre in Reproductive Science, University of Newcastle, Callaghan, 2308 AUS

[2]Institute for Molecular Bioscience, University of Queensland, Brisbane, 4072, AUS

[3]Telomere Length Regulation Group, Children's Medical Research Institute, University of Sydney, Westmead, 2145, AUS

[4]Anatomy and Neuroscience, University of Melbourne, Parkville, 3010 AUS

[5]Institute for Molecular Bioscience, University of Queensland, Brisbane, 4072, AUS

[6]School of Biological Sciences, University of Auckland, Auckland 1142, New Zealand

[*] ***Corresponding author;*** Dr. Jessie Sutherland

School of Biomedical Science & Pharmacy, University of Newcastle, University Drive, Callaghan, NSW 2308, Australia

Phone: +61 2 49138735

E-mail: jessie.sutherland@newcastle.edu.au

Running heading: *MSI2 regulation of mouse spermatogenesis*

Keywords:

- **MSI2**
- **Gametogenesis**
- **Testes**
- **RBP**
- **Spermatid**

Figures: 5 Tables: 3

Abstract

RNA-binding proteins (RBP) are important facilitators of post-transcriptional gene regulation. We have previously established that nuclear overexpression of the RBP Musashi-2 (MSI2) during male germ cell maturation is detrimental to sperm cell development and fertility. Herein we determine the genes and pathways impacted by the upregulation of *Msi2*. Microarray analysis and qPCR confirmed differential gene expression in factors fundamental to the cell cycle, cellular proliferation, and cell death. Similarly, comparative protein expression analysis via iTRAQ, immunoblot, and immunolocalisation, identified differential expression and localisation of important regulators of transcription, translation, RNA processing, and spermatogenesis. Specifically, the testis-expressed transcription factor, *Tbx1*, and the piRNA regulator of gamete development, *Piwil1,* were both found to be targeted for translational repression by MSI2. This study provides key evidence to support a fundamental role for MSI2 in post-transcriptional regulation during male gamete development.

Introduction

RNA binding proteins (RBPs) are essential for post-transcriptional regulation, expressed throughout the body, thus providing a common means of governing gene expression. An essential role of RBPs in controlling spermatogenesis, the process of gamete development in the testes, is well established (Idler and Yan, 2012). RBPs are proposed to be responsible for the extensive post-transcriptional modifications events that occur throughout the proliferation and differentiation of male germ cells, during extended periods of transcriptional cessation (Venables and Eperon, 1999). However, only recently, have the Musashi family of RBPs emerged as key molecules in spermatogenesis (Sutherland et al., 2015a).

In mammals, there are two Musashi family members: MSI1 and MSI2. Previously implicated in regulating cellular proliferation and cell fate determination (de Andrés-Aguayo et al., 2011; Kharas et al., 2010; Sakakibara et al., 2002), MSI2 has emerging roles in hematopoietic stem cell function

(Fujiwara et al., 2016; Park et al., 2014; Park et al., 2015). Furthermore, up-regulation of MSI2 has been associated with brain tumour growth (Cox et al., 2013), leukaemia progression (Lu et al., 2015; Mu et al., 2013; Thol et al., 2013), and, more recently, in lung and pancreatic cancer metastasis (Guo et al., 2016; Kudinov et al., 2016).

The MSI family is differentially expressed throughout mammalian spermatogenesis (Sutherland et al., 2014), with MSI1 a key regulator of the spermatogonial stem cell population (Sutherland et al., 2015b). However, the functional role of MSI2 during male gamete development is undetermined. We previously produced a transgenic mouse model (TgMsi2) of *Msi2* overexpression to establish whether MSI2 had any capacity, independent of MSI1, to regulate male fertility during post-transit spermatogonial amplification in spermatogenesis. This mouse model exhibited normal MSI2 localisation patterns (Fig. 1A & Fig. 1B) but the overexpression induced post meiotic germ cell arrest in the haploid spermatid population, resulting in a sterile phenotype (Sutherland et al., 2014).

In the present study, we establish the consequences of MSI2 overexpression on global gene and protein levels in isolated spermatogenic cells using microarray and iTRAQ analyses. The results emphasise the role of MSI2 in key biological functions including cellular growth and proliferation, cancer, RNA processing, translation, and spermatogenesis. By exploration of putative MSI2 action in the testis, we identified two, novel, spermatogenic-specific, RNA-binding targets in male germ cells: *Piwili1* and *Tbx1*. Utilising these targets, we demonstrate a potential action of MSI2 in the control of precursor mRNA (pre-mRNA) via translational repression. These findings support an essential role for MSI2 in post-transcriptional regulation during male gamete development, and highlight the important function(s) of RBPs in gametogenesis and fertility.

Materials & Methods

Animals: Use of animals for this study was approved by the University of Newcastle and University of Queensland Animal Care and Ethics Committees. All animals were maintained according to the recommendations prescribed by the ACEC. Prior to dissection, animals were euthanized via CO2 asphyxiation in accordance with ACEC directives.

Transgenic Mouse (TgMsi2) Production: The full-length 1.04 kb *Msi2* cDNA sequence (bases #140 to #1180) was overexpressed using the germ-cell specific promoter, the C4 isozyme of lactate dehydrogenase, *Ldhc4,* on a B6xCBA F2 background, with transgenic mice by genomic-PCR analysis, as previously described (Sutherland et al., 2014).

Spermatocyte and spermatid isolation: Spermatocytes and spermatids were isolated by loading 2 adult (>PND60) dissociated testes onto a 2-4% continuous bovine serum albumin (BSA) gradient (Sutherland et al., 2014). Briefly, testes were isolated, de-capsulated, and incubated for 15 min each in 0.5 mg/ml collagenase/DMEM with agitation and then in 0.25% trypsin/EDTA in DMEM. Tubules were dissociated manually by pipetting and washed in 0.5% BSA in DMEM by centrifugation. Cell pellets were resuspended in DMEM and filtered twice through a 70 µm membrane, then separated over a BSA gradient. Purified germ cells were identified by *Arachis hypogaea* lectin staining of the developing acrosome for spermatocytes and spermatids. Acrosome staining was performed as follows: cells were fixed for 10 min in ice-cold methanol and dried onto slides. Slides were incubated with 1 mg/ml lectin for 15 min, washed twice in PBS, and mounted in 10% Mowiol 4–88 with 30% glycerol in 0.2 M Tris (pH 8.5) with 2.5% 1,4-diazobicyclo-(2.2.2)-octane (DABCO). Cells were categorized based on both size and lectin staining pattern: spermatocytes exhibited relatively diffuse staining localized to a region representing the early stages of acrosome development, and spermatids were scored based on distinct labelling of the developing and elongating acrosome. Spermatocyte fractions were 65–70% pure with contaminating cells largely consisting of early

spermatocytes. Spermatids were 85–95% pure with contaminating cells consisting of late spermatocytes. Following separation, isolated cells were counted then washed in sterile PBS.

RNA extraction: Total RNA isolation was performed using two rounds of a modified acid guanidinium thiocyanate–phenol–chloroform protocol followed by isopropanol precipitation. Cytoplasmic and nuclear RNA separation was performed using a commercially available purification kit with the protocol described for lifted cells (Norgenbiotek).

Reverse Transcription PCR (RT-PCR) and Quantitative PCR (qPCR): Reverse transcription was performed as previously described (Sobinoff et al., 2013), or alternatively for nuclear and cytoplasmic separated RNAs using maxima first strand cDNA synthesis kit (Thermo Scientific). Total RNA was treated with DNase prior to reverse transcription to remove genomic DNA. Reverse transcription reactions were verified by *B-actin* RT-PCR using cDNA amplified with GoTaq Flexi (Promega). QPCR was performed using SYBR Green GoTaq qPCR master mix (Promega) according to manufacturer's instructions on LightCycler 96 SW 1.0 (Roche). For primer sequences see Supplemental Figure S1. QPCR reactions were performed and quantified as previously described (Sutherland et al., 2015b), with QPCR data was normalized to the house-keeping control *peptidylprolyl isomerase A (Ppia).*

Histomorphological Preparation and Immunohistochemistry Analysis: Whole mouse isolated testes were placed in Bouin's fixative for 12-24 h, washed in 70% ethanol, paraffin embedded and serially sectioned (4µm thick), throughout the entire testes. Sections were prepared and probed with antibodies specific for: Musashi-2 (MSI2, ab50829, Abcam), PCNA (PCNA, NA03T, Merck KGaA), Matrin-3 (MATR3, ab151714, Abcam), Nucleolin (NCL, ab22758, Abcam), DAZAP1 (NBP1-82741, Novus biologicals), PIWIL1 (ab12337, Abcam/MABE895, Millipore), PIWIL2 (ab3674, Abcam), SFPQ (ab11825, Abcam), YBX2 (PAB19295, Abnova), visualised with 10µg/mL fluorescently-conjugated

secondary antibody (goat anti-rabbit 555) for 1.5h at room temperature, washed, and counter-stained with 4'-6-Diamidino-2-phenylindole (DAPI), as previously described (Sutherland et al., 2015b). A Rabbit isotype control (#31235, Invitrogen) was used on each sample as a control for non-specific staining. Very faint non-specific IgG staining was observed in a small number of cells when incubated at 29µg/ml, well above the concentration of any primary target specific antibodies tested (Supplemental Figure S2).

Protein Extraction and Immunoblotting: Protein was extracted using ~300µl RIPA lysis buffer (150mM sodium chloride, 0.5% sodium deoxycholate, 1.0% Triton-X, 0.1% SDS, 50mM Tris, pH 8.0, Protocease protease inhibitor (GBiosciences St. Louis, MO, USA)) per 5 mg of cells or tissue. Protein concentration was estimated using a Pierce BCA Protein Assay Kit (Thermo Scientific). Immunodetection was conducted using primary antibodies previously described in Immunohistochemistry protocol, alongside SPESP1 (ab72672, Abcam), ZP3R (LS-C83508, LSbio), TM9SF2 (HPA005657, Sigma), and either GAPDH (G9545, Sigma) or α-Tubulin as a loading control (Tubulin, T5168, Sigma-Aldrich). Labelled antibodies were detected with Amersham ECL Western Blotting Detection Reagents (GE Healthcare UK Limited, Buckinghamshire, UK), with the results recorded using a cooled charge-coupled device camera system (Fuji-LAS-4000, Fujifilm Life Science Systems). Signal intensities of protein bands were quantitated where required using Fujifilm Multigauge software, v3.0.

Microarray Analysis: Total RNA (approximately 3 µg) was isolated from 4 TgMsi2 and 4 paired Wildtype (Wt) control adult testes using a QIAGEN RNeasy Mini Kit (Hilden, Germany). RNA was prepared for microarray analysis at the Australian Genome Research Facility (AGRF). Statistically significant genes with more than a 1.5-fold difference in gene expression ($p<0.05$) were then analysed using Ingenuity Pathways Analysis (Ingenuity Systems, Redwood City, CA) software to identify the top global molecular networks and primary biological functions and diseases affected by

Msi2 overexpression. The data discussed in this publication have been deposited in NCBI's Gene Expression Omnibus and are accessible through GEO Series accession number: GSE59358.

Proteomic analysis (iTRAQ): Isolated round spermatid protein from TgMsi2 and Wt littermates (N=2) were obtained for proteomic studies. The proteins were labelled at the Australian Proteome Analysis Facility (APAF) using the iTRAQ technique and separated by both reverse-phase and strong cation exchange HPLC AND NanoLC ESI MS/MS data acquisition. The experimental data was submitted to ProteinPilot for processing with the detected protein threshold set as larger than 1.3 (> 95% confidence), as detailed in (Rhein et al., 2009). Samples were compared via 4-way analysis, with the final list of differentially expressed proteins composed of targets with a geometric mean <0.83 or >1.2 with a combined p-value using Stouffer's method that was <0.05.

RNA-Immunoprecipitation: RNA-IP was performed on pooled collections of round spermatids from control adult mice (~$1x10^7$ cells/RNA-IP) using the Magna RIP™ RNA-Binding Protein Immunoprecipitation Kit and Musashi-2 RIPAb+ RIP Validated Antibody (Millipore Merk). Eluted target RNAs underwent reverse transcription and were analysed via qPCR.

Microscopy: All histological preparations were observed on an Axio Imager A1 epifluorescent microscope (Carl Zeiss MicroImaging Inc, Thornwood, NY) under fluorescent optics and pictures taken using an Olympus DP70 microscope camera (Olympus America, Centre Valley, PA).

Statistics: Statistical analysis was performed using JMP11 analysis software (SAS, Buckinghamshire, UK). All experiments were biologically replicated independently a minimum of 3 times, based on power of analysis. The majority of datasets presented a positively or negatively skewed distribution for which non-parametric Wilcoxon/Kruskal-Wallis testing was administered. In figures * denotes statistical significance, specifically; ***p<0.001, **p<0.01 *p<0.05.

Results

Effects of Musashi-2 overexpression on gene expression during spermatogenesis

MSI2 is normally expressed during spermatogenesis in spermatocyte and spermatid germ cells, and in the somatic Sertoli and Leydig cells, throughout post-natal testicular development in mice, with similar localisation observed in human testes (Sutherland et al., 2014). We developed a germ cell specific transgenic mouse model designed to ectopically overexpress isoform 1 of *Msi2* in the nucleus of meiotic spermatocytes and post-meiotic round spermatids. The MSI2 protein expression in our transgenic *Msi2* over-expression model (TgMsi2) replicated the physiological localisation pattern of MSI2. However, relative expression levels of both mRNA and protein were significantly enriched in spermatocyte and spermatid germ cells (Sutherland et al., 2014). Phenotypically, male TgMsi2 mice are sterile, producing spermatozoa with severe morphological and functional defects. In these mice, the post-meiotic spermatid germ cell population was the most significantly impacted (Sutherland et al., 2014).

To determine the genes and cellular signalling pathways affected in *Msi2* overexpression, comparative microarray analysis was performed on adult (PND60) whole testis messenger RNA that had been isolated from TgMsi2 mice and control Wildtype (Wt) littermates (N=4).

Overexpression of *Msi2* during spermatogenesis, had a significant impact on the adult testicular transcriptome, with over 700 genes differently expressed (DE) ($p<0.05$, fold change $>\pm1.5$), equating to approximately 2.7% of all array transcripts assessed (Supplemental Figure S3 A), with 58% of DE genes up regulated. Ingenuity Pathway Analysis (IPA) analyses identified the top five global molecular networks affected as: cell death, drug metabolism, cell morphology, cellular growth and proliferation, and the cell cycle. Analysis of molecular and cellular function, also using IPA, revealed the top ten biological functions and diseases ranked in order of the total number of DE genes (Supplemental Figure S3 B). The majority of DE genes for each functional classification were

upregulated in TgMsi2 testis, a large percentage of which were implicated in cancer (26%), cell death (21%), cellular growth and proliferation (20.5%), and reproductive system disease (17%).

Expression of the 12 most differentially expressed genes in the microarray data set was validated using qPCR (Table 1). Similar mRNA expression profiles were observed for all DE genes analysed, confirming the microarray data. The primary roles and functions of these genes were categorised into cellular proliferation and differentiation (*Timp1, Lrg1, Robo4, Rbp1, Gdf9, Sec23A,* and *Adipoq*) cellular trafficking (*Lrg1, Lcn2, Rbp1,* and *Sec23A*), reproductive processes and embryonic development (*Timp1, Robo4, Rbp1, Tbx1, Theg, Gdf9, HoxC9* and *Adam30*) and spermatogenesis (*Theg* and *Adam30*).

Analysis of potential MSI2-mRNA target Tbx1

Following the functional analysis of the DE genes in the TgMsi2 testis microarray, we determined that the transcription factor, *Tbx1* was suitable for further analyses based on published data. Specifically, TBX1 is known to be responsible for the control of embryo development and organogenesis (Takashima and Suzuki, 2013), with a role during spermatogenesis development in trout (Yano et al., 2011).

Immunolocalisation of TBX1 in adult mouse testis (Wt) indicated that TBX1 protein expression occurs primarily in spermatocytes with reduced expression in spermatids (Fig. 1A). In the TgMsi2 testes, TBX1 exhibited markedly reduced germ cell expression (Fig. 1A) and this was verified by immunoblot and densitometry analysis of fold change in purified spermatocyte (-1.51) and spermatid (-1.73) protein, relative to Wt (Fig. 1B). Conversely, qPCR analysis of *Tbx1* in TgMsi2 isolated germ cells, indicated a significant up-regulation of mRNA in spermatocytes (+8.08, $p<0.05$) and a similar trend in spermatids (+5.07, $p=0.06$), that was consistent with the results of our whole testis microarray (Fig. 1B & Table 1).

These findings indicated that *Tbx1* could be a direct mRNA target of MSI2. The proposed MSI2-mRNA binding interactions are further supported by the identification of five multiple Musashi core recognition and binding sequences (UAG) in the *Tbx1* 3' UTR (Supplemental Figure S4). (Zearfoss et al., 2014). To verify this interaction, RNA-immunoprecipitation (RNA-IP) was performed using dissociated whole adult mouse testis cells, and indicated significantly enriched *Tbx1* mRNA expression (+3.51, $p<0.05$) in MSI2-IP, compared to the control-IP and sample input, supporting a putative MSI2 protein- *Tbx1* mRNA interaction (Fig. 1C).

Conversely, qPCR for *Msi1,* as a predicted negative control, and *Numb,* as a previously predicted MSI2 mRNA target (by similarity (Ito et al., 2010; Okano et al., 2005)), revealed no significant enrichment of these mRNAs in the MSI2 RNA-IP, indicating that there is no interaction of MSI2 with either of these mRNAs in the mouse testis (Supplemental Figure S5).

Effects of Musashi-2 overexpression on spermatid proteome

The microarray analyses established global changes in mRNA expression resulting from the overexpression of *Msi2*, and enabled the identification of a novel MSI2 binding target in *Tbx1* mRNA. However, to define a role for MSI2, in the post-transcriptional regulation of the male germline, it was necessary to characterise *Msi2* overexpression specifically within testis germ cells. We have previously established that *Msi2* overexpression in the developing testes primarily impacted post meiotic spermatid germ cell development, significantly increasing DNA damage and apoptosis (Sutherland et al., 2014). To determine the overall effect of *Msi2* overexpression on the spermatid proteome, analysis of differential protein expression of spermatids purified from adult TgMsi2 mice and matched Wt littermates was undertaken.

Comparative isobaric Tag for Relative and Absolute Quantitation (iTRAQ), via two-dimensional nano-liquid chromatography (2D-nanoLC), electrospray ionization (ESI) mass spectrometry (MS/MS),

confirmed 206 up-regulated and 232 down-regulated proteins in TgMsi2 spermatids, representing 17% of the total 2501 proteins identified (Supplemental Figure S6 A). The previously characterised biological functions of these DE proteins (IPA) included transcriptional control, cell cycle regulation and cellular proliferation, translation, apoptosis, RNA splicing/processing, and spermatogenesis (Supplemental Figure S6 B).

Of these DE proteins, 65 (2.6%) were significantly altered ($p \leq 0.05$, fold change $>\pm 1.2$), with 58% down-regulated (Supplemental Figure S7). Table 2 summarises the twenty most differentially expressed proteins IDs. Functionally, these proteins were categorised as either RNA processing (MSI2, DDX21, PIWIL2, YBX2, PIWIL1, and DAZAP1, NCL, LA, MATR3, and MEX3D) and/or spermatogenesis (MSI2, DDX21, PIWIL2, YBX2, PIWIL1, and DAZAP1, RNLS, PBP2, CST8, PCNA, DPEP3, DNAH3, TM9SF2, ACRBP, ZP3R, and SPESP1). Validation of iTRAQ results was achieved through immunoblot analysis and densitometry of ten selected proteins, together with MSI2 as a positive control (Table 2, Supplemental Figure S8). Similar up and down regulated protein expression patterns were confirmed for all of the targets analysed, supporting the iTRAQ analysis.

Of the significantly up-regulated proteins, PCNA, PIWIL2, and NCL were of particular interest; given their identified roles in DNA replication and DNA damage response, meiotic differentiation of spermatocytes and piRNA regulation, and post-transcriptional modifications, respectively (Ginisty et al., 1999; Kuramochi-Miyagawa et al., 2004; Maga and Hübscher, 2003). Consequently, protein localisation of these three proteins was assessed, via immunolocalisation, in adult testis sections. All three of the proteins showed increased expression in the nuclei of spermatocytes and spermatids of TgMsi2 testes compared to Wt controls (Fig. 2A). Assessment MATR3, DAZAP1, and YBX2 protein localisation using immunolocalisation in adult testis sections, was also undertaken. Selection of these down-regulated proteins was due to demonstrated important roles in mRNA regulation and RNA binding (Skowronska-Krawczyk et al., 2014; Vera et al., 2002; Yang et al., 2007). Decreased

MATR3, DAZAP1, and YBX2 protein expression was observed in TgMsi2 spermatids, compared to Wt controls (Fig. 2B). In Wt testes, MATR3 and DAZAP1 exhibited spermatid nuclear localisation, while YBX2 was expressed in the cytoplasm.

It is important to note that there was limited overlap between the microarray DE genes the iTRAQ DE proteins with only three common identities (GPD2, TM9SF2, and ZP3R). TM9SF2 and ZP3R were similarly significantly down-regulated in TgMsi2 animals at a transcript level in the whole testis microarray (-1.52 and -1.59, respectively) and at the protein level in the round spermatid only iTRAQ (-1.57 and -2.51, respectively). In contrast, GPD2 was observed to be decreased in TgMsi2 animals at a transcript level in the whole testis microarray (-1.54, $p<0.001$) and increased at a protein level in the iTRAQ (+1.31, $p<0.001$), similarly qPCR analysis of G*pd2* expression in round spermatids only, also indicated a decrease in transcript levels (-1.62, N.S.), (Table 3). The lack of homology between our two analyses highlights the limitations of using whole testis rather than isolated germ cells for microarray analysis. Consequently, this directed us towards the exploration other DE proteins identified in the TgMsi2 iTRAQ analysis at the mRNA level through qPCR of isolated spermatids.

Effects of Musashi-2 overexpression on mRNA levels in spermatids

To establish a direct correlation between the over-expression of *Msi2* and the altered protein expression and localisation in the spermatids, mRNA transcript levels were analysed. QPCR analysis for the top ten significantly altered proteins identified from the TgMsi2 spermatid iTRAQ analysis was performed. Expression was compared to purified spermatids from cell number matched Wt controls (Table 3).

For the majority of the genes analysed, mRNA expression remained unchanged (*Pcna, Matr3, Ybx2,* and *Spesp1*), or not significantly changed (*Ncl* and *Zp3r*) (Table 3). Two proteins identified, DAZAP1 and PIWIL2, however did demonstrate significantly altered mRNA levels to a similar degree. Levels of

mRNA and protein of the spermatogenesis RBP, DAZ-associated protein 1 (*Dazap1*), were decreased in TgMsi2 spermatids (Table 3). In contrast, the piRNA pathway component and regulator of spermatogenesis, Piwi-like protein 2 (*Piwil2),* exhibited increased mRNA levels and protein expression in spermatids, as did *Msi2* (positive control) (Table 3). The positive correlation of both the mRNA and the protein expression indicates that the observed increase or decrease in protein is directly related to changes introduced at the mRNA level.

Interestingly, Piwi-like protein 1 (*Piwil1*), was the only iTRAQ ID analysed that exhibited opposing mRNA and protein expression, that is the mRNA level increased (+1.79 fold, $p<0.05$), whilst the protein level decreased (-1.35 fold, $p<0.001$), compared to the Wt control, in TgMsi2 spermatids. In the 3' UTR of *Piwil1*, we identified 16 Musashi core recognition sequences, confirming its potential as a MSI2 binding target (Supplemental Figure S4). Consequently, PIWIL1 was investigated as a putative RNA binding target of MSI2.

Analysis of potential MSI2-mRNA target Piwili1

PIWIL1 is member of the Piwi subfamily of Argonaute proteins, responsible for the biogenesis and functioning of a specialised class of gonad-specific noncoding RNAs: Piwi-interacting RNAs (piRNAs) (Grivna et al., 2006; Thomson and Lin, 2009). PIWI proteins act in a complex with piRNAs to mediate the repression of mutagenic transposable elements during meiosis to the protect germline (Pillai and Chuma, 2012). *Piwil1* null male mice are infertile and exhibit a testicular phenotype similar to TgMsi2 mice, with arrested spermatogenesis at the spermatid stage (Deng and Lin, 2002). Functionally, PIWIL1 mediates the necessary degradation of a large population of mRNAs in late spermiogenesis (Gou et al., 2014), prior to spermiation.

Immunolocalisation of PIWIL1 in adult mouse testis (Wt) demonstrated cytoplasmic expression in spermatids (Fig. 3A). In TgMsi2 testis sections, PIWIL1 expression was either lost or visibly reduced in spermatids (Fig. 3A). Immunoblot and densitometry examination of isolated spermatids identified a

slight, but non-significant, reduction in PIWIL1 protein expression (-1.13, NS) (Fig. 3B). In contrast, qPCR analysis of *Piwil1* in TgMsi2 isolated cells indicated a significant up-regulation of mRNA in the spermatids (+1.79, $p<0.05$), consistent with the results of the whole testis microarray (Fig. 3B & Table 3).

RNA-IP was utilised again to determine if *Piwil1* was a direct MSI2 binding target. Using qPCR, MSI2 RNA-IP analysis of dissociated adult mouse testis confirmed significantly enhanced *Piwil1* mRNA (+2.54, $p\leq0.01$) when compared to control-IP and sample input (Fig. 3C), thus, confirming a direct interaction between MSI2 and *Piwil1* mRNA. With *Tbx1* and *Piwil1* confirmed as MSI2-mRNA targets, both of which exhibited evidence of translational repression, we then sought to determine a mechanism through which MSI2 might control target expression.

Functional role of MSI2 in mRNA regulation

The mechanisms through which RBPs exert post-transcriptional control are limited to the functional capabilities of the specific RBP, in addition to its specific sub-cellular localisation (Glisovic et al., 2008). As MSI2 expression is confined to the nucleus during spermatogenesis (Sutherland et al., 2014), there is little evidence to support its interaction with translational machinery in the cytoplasm as a potential mechanism of expression repression. Consequently, we predicted a role for MSI2 in nuclear mRNA processing and regulation events e.g. splicing, polyadenylation, and mRNA maturation. Therefore, if MSI2 is indeed targeting *Piwil1* and *Tbx1* mRNA, as hypothesised, the alterations that were observed in mRNA expression of these potential targets must be occurring in the nucleus of spermatids.

To better clarify the observed uncoupled transcript and protein expression of the putative MSI2 mRNA targets, *Piwil1* and *Tbx1*, we undertook comparative qPCR of cytoplasmic versus nuclear mRNA, using purified TgMsi2 spermatids and cell number matched Wt control spermatids. Total RNA

content was measured using pan precursor-mRNA and mature mRNA specific primers and measured relative to the steady-state control mRNA of *Ppia*. Subtle enrichment of nuclear expression, relative to cytoplasmic expression, of both *Piwil1* (1.2 fold, p=0.19) (Fig. 4A), and *Tbx1* (1.5 fold, p=0.24) RNA (Fig. 4B), was observed in TgMsi2 spermatids (N=3). These data suggest that the decreased protein expression of PIWIL1 and TBX1, observed in TgMsi2 spermatids, may be due to a decrease in mature mRNA present within the cytoplasm. If indeed MSI2 is responsible for retaining RNA within the nucleus, we predict that translation may be repressed as a result of incomplete processing of pre-mRNA, or prevention of mature mRNA export. (Figure 5).

Discussion

The Musashi family of RNA binding proteins are required in key developmental processes wwith established roles in stem cell proliferation and differentiation (Okano et al., 2005), cell cycle regulation (MacNicol et al., 2011), and haematopoiesis (de Andres-Aguayo et al., 2012; de Andrés-Aguayo et al., 2011). Furthermore, Musashi is frequently upregulated in a variety of disease conditions, consistently as a gene of interest in multiple stem cell cancers (Glazer et al., 2012; Götte et al., 2008; Sutherland et al., 2013; Todaro et al., 2010). Recently, we have established that Musashi is important to the processes of male and female gamete development (Sutherland et al., 2014; Sutherland et al., 2015b; Sutherland et al., 2015c). - Using a transgenic mouse model, we have previously demonstrated that germ cell-specific overexpression of *Msi2*, but not *Msi1*, is responsible for male infertility, with no evidence of MSI1 rescue (Sutherland et al., 2014). In this study, we first utilised comparative gene and protein expression analyses to determine the impact of *Msi2* overexpression on testicular germ cell development and, identify a potential mechanism for the action of MSI2 in post-transcriptional regulation.

The differentially expressed (DE) genes from our microarray analysis supported the known role(s) of Musashi, in cancer, gastrointestinal disease, cellular growth and proliferation, and neurological

disease. Also identified were a large number of DE genes with confirmed roles in transcription, cellular trafficking, and reproductive processes. None of the previously characterised mRNA targets of MSI2 were found to be differentially expressed, including *Numb* and *Notch* (Griner and Reuther, 2010; Ito et al., 2010; Nishimoto and Okano, 2010). And, similar to previous findings in hematopoietic stem cells (Kaeda et al., 2015; Park et al., 2014), a direct MSI2-*Numb* interaction in the mouse testes was unsupported by RNA-IP. Indicating an active role for MSI2 in the post-transcriptional regulation of genes essential to spermatogenesis, independent of NUMB-NOTCH signalling.

The iTRAQ analysis of global protein expression revealed aberrant expression of a number of key proteins sharing common biological functions with those identified in our microarray study: cell death, cell cycle, and cellular growth and proliferation, and spermatogenesis. Whilst also highlighting the processes of splicing and mRNA processing. We predicted that MSI2, acting as nuclear expressed RBP, would function in transcript maturation through binding and regulating pre-mRNA (Halbeisen et al., 2008), and frequently work in dynamic complexes containing multiple RBPs (Nguyen-Chi and Morello, 2011). Accordingly, our iTRAQ analysis revealed a high number of DE proteins with identified roles in RNA binding and regulation.

The detailed analysis of TgMsi2 transcriptome and proteome uncovered two testis-specific MSI2-RNA binding targets in *Tbx1* and *Piwil1*, with evidence for their translational repression in spermatids, via a MSI2-mRNA binding interaction. The implications of MSI2-mediated PIWIL1 repression include a reduction in Piwi-mediated genome protection, resulting in increased transposon activity and higher rates of mutagenesis (Pillai and Chuma, 2012; Siomi et al., 2011). Additionally, we predict a severe retardation of the PIWIL1-mediated decay of multiple mRNAs, necessary for normal sperm development (Gou et al., 2014). Furthermore, TBX1 is an essential developmental transcription factor with a likely role in early spermatogenesis (Yano et al., 2011).

Specifically, *in vivo* studies of *Tbx1* loss-of-function in mice have demonstrated a wide range of developmental anomalies, resulting in embryonic or perinatal lethality (Jerome and Papaioannou, 2001; Zhang and Baldini, 2008). Supporting the published studies, our TgMsi2 mouse model demonstrated downregulation of TBX1, during spermatogenesis, with disrupted differentiation and cell division during germ cell development. However, detailed molecular analysis of downstream targets is necessary to confirm if translation inhibition of PIWIL1 and TBX1 is causing the TgMsi2 testicular phenotype observed. .

The mechanism of MSI2-driven post-transcriptional gene regulation, as evidenced via uncoupled transcript and protein expression, has been recently established in human HSCs (Rentas et al., 2016). We therefore hypothesised that the observed decreases in protein expression of TBX1 and PIWIL1 may be due the retention of their RNAs within the cytoplasm. However, our functional analysis of the mRNA expression of the hypothesised targets identified a subtle but not-significant increase of both *Tbx1* and *Piwil1* in the nucleus of spermatocytes and spermatids, under conditions of MSI2 overexpression, further confirmation is required in order to determine if indeed nuclear accumulation of these pre-mRNAs is occurring. Quantitative RNA *in situ* hybridisation alongside splicing and polyadenylation assays may also clarify the precise mechanism utilised by MSI2.

In summary, this study has identified a functional role for MSI2 in the post-transcriptional regulation of target gene expression during spermatogenesis, independent to that of MSI1. Exemplifying the requisite need to investigate the role of RNA binding proteins, utilising knowledge of their subcellular expression within the tissues of interest.

Acknowledgements

Financial assistance provided to EAM and GRH by the Australian Research Council, National Health and Medical Research Council and Hunter Medical Research Institute. Additional support was

provided the ARC Centre of Excellence in Biotechnology (EAM, PK and GRH). JMS was supported by an Australian Postgraduate Award PhD scholarship (2012-2015). The authors declare no conflict of interest.

References

Arumugam K, MacNicol MC, MacNicol AM. 2012. Autoregulation of Musashi1 mRNA translation during Xenopus oocyte maturation. Molecular reproduction and development 79(8):553-563.

Asai R, Okano H, Yasugi S. 2005. Correlation between Musashi-1 and c-hairy-1 expression and cell proliferation activity in the developing intestine and stomach of both chicken and mouse. Development, growth & differentiation 47(8):501-510.

Bettegowda A, Wilkinson MF. 2010. Transcription and post-transcriptional regulation of spermatogenesis. Philosophical Transactions of the Royal Society B: Biological Sciences 365(1546):1637.

Byers RJ, Currie T, Tholouli E, Rodig SJ, Kutok JL. 2011. MSI2 protein expression predicts unfavorable outcome in acute myeloid leukemia. Blood 118(10):2857-2867.

Cox JL, Wilder PJ, Gilmore JM, Wuebben EL, Washburn MP, Rizzino A. 2013. The SOX2-interactome in brain cancer cells identifies the requirement of MSI2 and USP9X for the growth of brain tumor cells. PloS one 8(5).

Cragle C, Macnicol AM. 2014. Musashi-directed translational activation of target mRNAs is mediated by the poly[A] polymerase, Germline Development-2. J Biol Chem 18:18.

de Andres-Aguayo L, Varas F, Graf T. 2012. Musashi 2 in hematopoiesis. Current opinion in hematology 19(4):268-272.

de Andrés-Aguayo L, Varas F, Kallin EM, Infante JF, Wurst W, Floss T, Graf T. 2011. Musashi 2 is a regulator of the HSC compartment identified by a retroviral insertion screen and knockout mice. Blood 118(3):554-564.

Deng W, Lin H. 2002. miwi, a murine homolog of piwi, encodes a cytoplasmic protein essential for spermatogenesis. Developmental cell 2(6):819-830.

Elliott DJ, Grellscheid SN. 2006. Alternative RNA splicing regulation in the testis. Reproduction 132(6):811-819.

Evans C, Noirel J, Ow SY, Salim M, Pereira-Medrano AG, Couto N, Pandhal J, Smith D, Pham TK, Karunakaran E, Zou X, Biggs CA, Wright PC. 2012. An insight into iTRAQ: where do we stand now? Anal Bioanal Chem 404(4):1011-1027.

Fujiwara T, Zhou J, Ye S, Zhao H. 2016. RNA-binding protein Musashi2 induced by RANKL is critical for osteoclast survival. Cell Death Dis 7:e2300.

Ginisty H, Sicard H, Roger B, Bouvet P. 1999. Structure and functions of nucleolin. Journal of cell science 112 (Pt 6):761-772.

Glazer R, Vo D, Penalva L. 2012. Musashi1: an RBP with versatile functions in normal and cancer stem cells. Frontiers in bioscience: a journal and virtual library 17:54.

Glisovic T, Bachorik JL, Yong J, Dreyfuss G. 2008. RNA-binding proteins and post-transcriptional gene regulation. FEBS letters 582(14):1977-1986.

Götte M, Wolf M, Staebler A, Buchweitz O, Kelsch R, Schüring A, Kiesel L. 2008. Increased expression of the adult stem cell marker Musashi-1 in endometriosis and endometrial carcinoma. The Journal of pathology 215(3):317-329.

Gou LT, Dai P, Yang JH, Xue Y, Hu YP, Zhou Y, Kang JY, Wang X, Li H, Hua MM, Zhao S, Hu SD, Wu LG, Shi HJ, Li Y, Fu XD, Qu LH, Wang ED, Liu MF. 2014. Pachytene piRNAs instruct massive mRNA elimination during late spermiogenesis. Cell Res 24(6):680-700.

Griner LN, Reuther GW. 2010. Aggressive myeloid leukemia formation is directed by the Musashi 2/Numb pathway. Cancer Biol Ther 10(10):979-982.

Grivna ST, Beyret E, Wang Z, Lin H. 2006. A novel class of small RNAs in mouse spermatogenic cells. Genes Dev 20(13):1709-1714.

Guo K, Cui J, Quan M, Xie D, Jia Z, Wei D, Wang L, Gao Y, Ma Q, Xie K. 2016. A novel KLF4-MSI2 signaling pathway regulates growth and metastasis of pancreatic cancer. Clin Cancer Res.

Halbeisen RE, Galgano A, Scherrer T, Gerber AP. 2008. Post-transcriptional gene regulation: from genome-wide studies to principles. Cellular and molecular life sciences : CMLS 65(5):798-813.

Idler RK, Yan W. 2012. Control of Messenger RNA Fate by RNA-Binding Proteins: An Emphasis on Mammalian Spermatogenesis. Journal of andrology 33(3):309-337.

Imai H, Chan EK, Kiyosawa K, Fu XD, Tan EM. 1993. Novel nuclear autoantigen with splicing factor motifs identified with antibody from hepatocellular carcinoma. The Journal of clinical investigation 92(5):2419-2426.

Ito T, Kwon HY, Zimdahl B, Congdon KL, Blum J, Lento WE, Zhao C, Lagoo A, Gerrard G, Foroni L. 2010. Regulation of myeloid leukaemia by the cell-fate determinant Musashi. Nature 466(7307):765-768.

Jerome LA, Papaioannou VE. 2001. DiGeorge syndrome phenotype in mice mutant for the T-box gene, Tbx1. Nature genetics 27(3):286-291.

Kaeda J, Ringel F, Oberender C, Mills K, Quintarelli C, Pane F, Koschmieder S, Slany R, Schwarzer R, Saglio G, Hemmati P, van Lessen A, Amini L, Gresse M, Vagge E, Burmeister T, Serra A, Carson A, Schwarz M, Westermann J, Jundt F, Dorken B, le Coutre P. 2015. Up-regulated MSI2 is associated with more aggressive chronic myeloid leukemia. Leukemia & lymphoma 56(7):2105-2113.

Kawahara H, Imai T, Imataka H, Tsujimoto M, Matsumoto K, Okano H. 2008. Neural RNA-binding protein Musashi1 inhibits translation initiation by competing with eIF4G for PABP. The Journal of Cell Biology 181(4):639.

Kharas MG, Lengner CJ, Al-Shahrour F, Bullinger L, Ball B, Zaidi S, Morgan K, Tam W, Paktinat M, Okabe R. 2010. Musashi-2 regulates normal hematopoiesis and promotes aggressive myeloid leukemia. Nature Medicine 16(8):903-908.

Kudinov AE, Deneka A, Nikonova AS, Beck TN, Ahn YH, Liu X, Martinez CF, Schultz FA, Reynolds S, Yang DH, Cai KQ, Yaghmour KM, Baker KA, Egleston BL, Nicolas E, Chikwem A, Andrianov G, Singh S, Borghaei H, Serebriiskii IG, Gibbons DL, Kurie JM, Golemis EA, Boumber Y. 2016. Musashi-2 (MSI2) supports TGF-beta signaling and inhibits claudins to promote non-small cell lung cancer (NSCLC) metastasis. Proceedings of the National Academy of Sciences of the United States of America 113(25):6955-6960.

Kuldau GA, Raju NB, Glass NL. 1998. Repeat-induced point mutations in Pad-1, a putative RNA splicing factor from Neurospora crassa, confer dominant lethal effects on ascus development. Fungal genetics and biology : FG & B 23(2):169-180.

Kuramochi-Miyagawa S, Kimura T, Ijiri TW, Isobe T, Asada N, Fujita Y, Ikawa M, Iwai N, Okabe M, Deng W, Lin H, Matsuda Y, Nakano T. 2004. Mili, a mammalian member of piwi family gene, is essential for spermatogenesis. Development 131(4):839-849.

Kuwako K, Kakumoto K, Imai T, Igarashi M, Hamakubo T, Sakakibara S, Tessier-Lavigne M, Okano H, Okano H. 2010. Neural RNA-binding protein Musashi1 controls midline crossing of precerebellar neurons through posttranscriptional regulation of Robo3/Rig-1 expression. Neuron 67(3):407.

Lu S, Mu Q, Yu M, Yin X, Chen J, Jin J. 2015. Overexpression of musashi2 is possibly associated with chemoresistance in T-cell acute lymphoblastic leukemia. Leukemia & lymphoma:1-3.

MacNicol MC, Cragle CE, MacNicol AM. 2011. Context-dependent regulation of Musashi-mediated mRNA translation and cell cycle regulation. Cell Cycle 10(1):39-44.

Maga G, Hübscher U. 2003. Proliferating cell nuclear antigen (PCNA): a dancer with many partners. Journal of Cell Science 116(15):3051-3060.

McLaughlin EA, Hime GR. 2011. Spermatids do it differently! Paip2a—the essential regulator of spermiogenesis? Asian Journal of Andrology 13(1):122-124.

Mu Q, Wang Y, Chen B, Qian W, Meng H, Tong H, Chen F, Ma Q, Ni W, Chen S. 2013. High expression of Musashi-2 indicates poor prognosis in adult B-cell acute lymphoblastic leukemia. Leukemia Research.

Nguyen-Chi M, Morello D. 2011. RNA-binding proteins, RNA granules, and gametes: is unity strength? Reproduction 142(6):803-817.

Nickerson P, Myers T, Clarke D, Chow R. 2011. Changes in Musashi-1 subcellular localization correlate with cell cycle exit during postnatal retinal development. Experimental eye research 92(5):344-352.

Nishimoto Y, Okano H. 2010. New insight into cancer therapeutics: Induction of differentiation by regulating the Musashi/Numb/Notch pathway. Cell research 20(10):1083-1085.

Okano H, Kawahara H, Toriya M, Nakao K, Shibata S, Imai T. 2005. Function of RNA-binding protein Musashi-1 in stem cells. Experimental cell research 306(2):349.

Park SM, Deering RP, Lu Y, Tivnan P, Lianoglou S, Al-Shahrour F, Ebert BL, Hacohen N, Leslie C, Daley GQ, Lengner CJ, Kharas MG. 2014. Musashi-2 controls cell fate, lineage bias, and TGF-beta signaling in HSCs. The Journal of experimental medicine 211(1):71-87.

Park SM, Gonen M, Vu L, Minuesa G, Tivnan P, Barlowe TS, Taggart J, Lu Y, Deering RP, Hacohen N, Figueroa ME, Paietta E, Fernandez HF, Tallman MS, Melnick A, Levine R, Leslie C, Lengner CJ, Kharas MG. 2015. Musashi2 sustains the mixed-lineage leukemia-driven stem cell regulatory program. The Journal of clinical investigation 125(3):1286-1298.

Pillai RS, Chuma S. 2012. piRNAs and their involvement in male germline development in mice. Dev Growth Differ 54(1):78-92.

Rentas S, Holzapfel N, Belew MS, Pratt G, Voisin V, Wilhelm BT, Bader GD, Yeo GW, Hope KJ. 2016. Musashi-2 Attenuates AHR Signaling to Expand Human Hematopoietic Stem Cells. Nature 532(7600):508-511.

Rhein V, Song X, Wiesner A, Ittner LM, Baysang G, Meier F, Ozmen L, Bluethmann H, Drose S, Brandt U, Savaskan E, Czech C, Gotz J, Eckert A. 2009. Amyloid-beta and tau synergistically impair the oxidative phosphorylation system in triple transgenic Alzheimer's disease mice. Proceedings of the National Academy of Sciences of the United States of America 106(47):20057-20062.

Sakakibara S-i, Nakamura Y, Satoh H, Okano H. 2001. Rna-binding protein Musashi2: developmentally regulated expression in neural precursor cells and subpopulations of neurons in mammalian CNS. The Journal of Neuroscience 21(20):8091-8107.

Sakakibara S, Nakamura Y, Yoshida T, Shibata S, Koike M, Takano H, Ueda S, Uchiyama Y, Noda T, Okano H. 2002. RNA-binding protein Musashi family: Roles for CNS stem cells and a subpopulation of ependymal cells revealed by targeted disruption and antisense ablation. Proceedings of the National Academy of Sciences of the United States of America 99(23):15194.

Siomi MC, Sato K, Pezic D, Aravin AA. 2011. PIWI-interacting small RNAs: the vanguard of genome defence. Nature reviews Molecular cell biology 12(4):246-258.

Skowronska-Krawczyk D, Ma Q, Schwartz M, Scully K, Li W, Liu Z, Taylor H, Tollkuhn J, Ohgi KA, Notani D, Kohwi Y, Kohwi-Shigematsu T, Rosenfeld MG. 2014. Required enhancer-matrin-3 network interactions for a homeodomain transcription program. Nature 514(7521):257-261.

Sobinoff A, Beckett E, Jarnicki A, Sutherland J, McCluskey A, Hansbro P, McLaughlin E. 2013. Scrambled and fried: Cigarette smoke exposure causes antral follicle destruction and oocyte dysfunction through oxidative stress. Toxicology and applied pharmacology 271(2):156-167.

Sutherland JM, Fraser BA, Sobinoff AP, Pye VJ, Davidson TL, Siddall NA, Koopman P, Hime GR, McLaughlin EA. 2014. Developmental expression of Musashi-1 and Musashi-2 RNA-binding proteins during spermatogenesis: analysis of the deleterious effects of dysregulated expression. Biology of reproduction 90(5):92.

Sutherland JM, McLaughlin EA, Hime GR, Siddall NA. 2013. The Musashi Family of RNA Binding Proteins: Master Regulators of Multiple Stem Cell Populations. Transcriptional and Translational Regulation of Stem Cells: Springer. p 233-245.

Sutherland JM, Siddall NA, Hime GR, McLaughlin EA. 2015a. RNA binding proteins in spermatogenesis: an in depth focus on the Musashi family. Asian J Androl.

Sutherland JM, Sobinoff AP, Fraser BA, Redgrove KA, Davidson TL, Siddall NA, Koopman P, Hime GR, McLaughlin EA. 2015b. RNA binding protein Musashi-1 directly targets Msi2 and Erh during early testis germ cell development and interacts with IPO5 upon translocation to the nucleus. FASEB J.

Sutherland JM, Sobinoff AP, Gunter KM, Fraser BA, Pye V, Bernstein IR, Boon E, Siddall NA, De Andres LI, Hime GR, Holt JE, Graf T, McLaughlin EA. 2015c. Knockout of RNA Binding Protein MSI2 Impairs Follicle Development in the Mouse Ovary: Characterization of MSI1 and MSI2 during Folliculogenesis. Biomolecules 5(3):1228-1244.

Takashima Y, Suzuki A. 2013. Regulation of organogenesis and stem cell properties by T-box transcription factors. Cellular and molecular life sciences : CMLS 70(20):3929-3945.

Thol F, Winschel C, Sonntag AK, Damm F, Wagner K, Chaturvedi A, Gohring G, Schlegelberger B, Lubbert M, Fiedler W, Kirchner H, Krauter J, Ganser A, Heuser M. 2013. Prognostic significance of expression levels of stem cell regulators MSI2 and NUMB in acute myeloid leukemia. Ann Hematol 92(3):315-323.

Thomson T, Lin H. 2009. The biogenesis and function of PIWI proteins and piRNAs: progress and prospect. Annu Rev Cell Dev Biol 25:355-376.

Todaro M, Francipane MG, Medema JP, Stassi G. 2010. Colon cancer stem cells: promise of targeted therapy. Gastroenterology 138(6):2151-2162.

Venables J, Eperon I. 1999. The roles of RNA-binding proteins in spermatogenesis and male infertility. Current opinion in genetics & development 9(3):346.

Vera Y, Dai T, Hikim AP, Lue Y, Salido EC, Swerdloff RS, Yen PH. 2002. Deleted in azoospermia associated protein 1 shuttles between nucleus and cytoplasm during normal germ cell maturation. J Androl 23(5):622-628.

Wang MH, Qin SY, Zhang SG, Li GX, Yu ZH, Wang K, Wang B, Teng MJ, Peng ZH. 2015. Musashi-2 promotes hepatitis Bvirus related hepatocellular carcinoma progression via the Wnt/beta-catenin pathway. Am J Cancer Res 5(3):1089-1100.

Wuebben E, Mallanna S, Cox J, Rizzino A. 2012. Musashi2 is required for the self-renewal and pluripotency of embryonic stem cells. PloS one 7(4):e34827.

Yang J, Morales CR, Medvedev S, Schultz RM, Hecht NB. 2007. In the absence of the mouse DNA/RNA-binding protein MSY2, messenger RNA instability leads to spermatogenic arrest. Biology of reproduction 76(1):48-54.

Yano A, Nicol B, Guerin A, Guiguen Y. 2011. The duplicated rainbow trout (Oncorhynchus mykiss) T-box transcription factors 1, tbx1a and tbx1b, are up-regulated during testicular development. Mol Reprod Dev 78(3):172-180.

Yeo G, Holste D, Kreiman G, Burge CB. 2004. Variation in alternative splicing across human tissues. Genome Biol 5(10):13.

Zearfoss NR, Deveau LM, Clingman CC, Schmidt E, Johnson ES, Massi F, Ryder SP. 2014. A Conserved Three-nucleotide Core Motif Defines Musashi RNA Binding Specificity. The Journal of biological chemistry 289(51):35530-35541.

Zhang Z, Baldini A. 2008. In vivo response to high-resolution variation of Tbx1 mRNA dosage. Hum Mol Genet 17(1):150-157.

Figure Legends

Figure 1: TBX1 in spermatogenesis, comparison of transcript and protein in TgMsi2 adult (PND60) male testis, and isolated germ cells.

A. Immunolocalisation of TBX1 on TgMsi2 round spermatids using TgMsi2 adult (PND60) testis sections and Wildtype littermates. Sections were fluorescently probed forTBX1 (red), counterstained with nuclear marker DAPI (blue), and visualized via epifluorescent microscopy. Scale bars denote 200um.

B. Summary table of *Tbx1*/TBX1 expression in TgMsi2 animals relative to Wt littermates. Column 1 describes sample, column 2 describes type of analysis performed, and column 3 details relative expression results in TgMsi2 sample relative to Wt Littermates. For qPCR: total RNA was isolated from TgMsi2 spermatocytes or spermatids and Wt littermates (N=3), reverse transcribed, and qPCR performed for *Tbx1*. For Western blot (WB): Immunoblots of TgMsi2 isolated cells (spermatocytes and spermatids) and Wt littermates (N=2), were probed for TBX1 and densitometry was performed on expression level relative to loading control.

C. MSI2 RNA immunoprecipitation of native dissociated adult mouse testis lysate from control mice (N=3). Eluted mRNAs were reverse transcribed, and qPCR performed with primers specific for *Tbx1*. Input sample is equivalent to 10% of total RNA lysate added to each IP. Control-IP denotes RNA-IP performed using rabbit IgG only. Data is presented as mean relative expression normalised to control-IP (set to 1) +SE.

Figure 2: Immunolocalisation of DE proteins identified in iTRAQ analysis on TgMsi2 round spermatids using TgMsi2 adult (PND60) testis sections and Wildtype littermates. Scale bars denote 100um.

A. Up-regulated IDs: Sections were fluorescently probed for, PCNA, PIWIL2, and NCL (red), counterstained with nuclear marker DAPI (blue), and visualized via epifluorescent microscopy.

B. Down-regulated IDs: Sections were fluorescently probed for; MATR3, DAZAP1, and YBX2 (red), counterstained with nuclear marker DAPI (blue), and visualized via epifluorescent microscopy.

Figure 3: PIWIL1 in spermatogenesis, comparison of transcript and protein in TgMsi2 spermatids.

A. Immunolocalisation of PIWIL1 in spermatids using TgMsi2 adult (PND60) testis sections and Wildtype littermates. Testis sections (N=4) were probed for PIWIL1 (red) and counterstained with DAPI (blue) acoridng to materials and methods. Labels on higher magnification images indicate spermatocytes (spc) and spermatids (spt). Scale bars denote 50µm.

B. Summary table of*Piwil1/*PIWIL1 expression in TgMsi2 purified spermatids relative to Wt littermates. For qPCR: total RNA was isolated from TgMsi2 spermatids and Wt littermates (N=3), reverse transcribed, and qPCR performed for *Piwil1*. For Western blot (WB): Immunoblots of TgMsi2 and WT spermatids (N=2), were probed for PIWIL1 and densitometry was performed on expression level relative to loading control.

C. MSI2 RNA immunoprecipitation of native dissociated adult mouse testis lysate from control mice (N=3). Eluted mRNAs were reverse transcribed, and qPCR performed with primers specific for *Piwil1*. Input sample is equivalent to 10% of total RNA lysate added to each IP. Control-IP denotes RNA-IP performed using rabbit IgG only. Data is presented as mean relative expression normalised to control-IP (set to 1) +SE.

Figure 4: qPCR analysis of *Piwil1* and *Tbx1* subcellular expression

A. QPCR analysis was performed on cytoplasmic versus nuclear extracted RNA from TgMsi2 testis cells and Wt littermates (N=3). Total RNA content was measured using pan pre-mRNA and mature mRNA specific primers for *Piwil1*, and compared relative to steady state control *Ppia*. Data is presented as average ratio of nuclear to cytoplasmic relative expression +SE (p=0.19).

B. QPCR analysis of total *Tbx1* RNA was performed on cytoplasmic versus nuclear extracted RNA from TgMsi2 testis cells and Wt littermates as described above (A) (p=0.24).

Figure 5: Model depicting potential MSI2 mechanism of action in TgMsi2 in spermatids. We have demonstrated the specific localisation of RNA binding protein MSI2 in the nucleus of spermatids (i). Through RNA immunoprecipitation, an interaction of MSI2 with *Tbx1* and *Piwil1* mRNA has been identified (ii). Using iTRAQ, immunoblot, and immunolocalisation, we have shown evidence for the regulation of TBX1 and PIWIL1 translation (iii).

Supplementary Figure Legends:

Supplemental Figure S1: Primers and sequences

Supplemental Figure S2: Immunofluorescence of Rabbit isotype control using TgMsi2 adult (PND60) testis sections and Wildtype littermates. Scale bars denote 50µm. A small amount of non-specific rabbit IgG was detected as indicated (→). All other conditions remained unchanged. Sections were

fluorescently probed with secondary antibody (red), counterstained with nuclear marker DAPI (blue), and visualized via epifluorescent microscopy.

Supplemental Figure S3: Microarray analysis of TgMsi2 adult mouse testes compared to Wt littermates (N=4).

A. The pie graph displays the total number of genes found on an Illumina Sentrix Mouse ref8v2 Beadchip, presented as positive hits (genes with a significant change in expression (>1.5-fold change, $p \leq 0.05$)) within the total number of transcripts analysed (array transcripts). The bar of pie represents the breakdown of up-regulated genes to down-regulated genes, identified in TgMsi2 testes.
B. The top 10 biological functions and diseases arranged in order of number of molecules identified as differentially expressed from microarray analysis. Threshold represents –log(p-value) set at 1.3. The number of up-regulated and down-regulated genes present for each data point are represented as a relative fraction of the y-axis value. Genes were analysed using Ingenuity Pathways Analysis (Ingenuity Systems) for molecular and cellular functions. Only those genes exhibiting a greater than 1.5-fold change in expression were categorised ($p \leq 0.05$). Note that some genes occur in multiple functional groups.

Supplemental Figure S4: Identification of MSI2 consensus sequence UAG in 3' UTR of Tbx1 and Piwil1. Figure shows 3' UTR of mouse Tbx1 and Piwil1 (sourced from Ensembl genome browser) with MSI2 binding sequence UAG (TAG) highlighted.

Supplemental Figure S5: MSI2 RNA-IP with adult mouse testis, qPCR for Msi1 and Numb.

A. RNA immunoprecipitation was performed using a MSI2 specific antibody bound to protein G magnetic beads to pull-down MSI2 protein binding partners in native dissociated adult mouse testis lysate from control mice (N=3). Eluted mRNAs were reverse transcribed, and qPCR performed with primers specific for Msi1. Input

sample is equivalent to 10% of total RNA lysate added to each IP. Control-IP denotes RNA-IP performed using rabbit IgG. Data is presented as mean relative expression normalised to control-IP (set to 1) +SE. (**p<0.01 denotes statistical significance).

B. Experiment as described above with qPCR performed using primers specific for Numb. Input sample is equivalent to 10% of total RNA lysate added to each IP. Control-IP denotes RNA-IP performed using rabbit IgG. Data is presented as mean relative expression normalised to control-IP (set to 1) +SE.(note: no statistical significance was found between groups).

Supplemental Figure S6: ITRAQ analysis of TgMsi2 adult mouse isolated spermatids compared to Wt littermates (N=2).

A. Summary of iTRAQ results. The pie graph displays the total number of proteins identified via 2D NanoLC ESI MS/MS data acquisition using the iTRAQ method, and the number of these considered to be differentially altered. The bar of pie represents the breakdown of up-regulated proteins to downregulated proteins, identified in TgMsi2 spermatids.

B. ITRAQ summary of the top six combined biological processes affected as a result of *Msi2* overexpression, arranged in order of number of differentially expressed proteins. The numbers of proteins in each group are shown in parentheses.

Supplemental Figure S7: DE proteins from comparative iTRAQ analysis of TgMsi2 round spermatids. Peptides.95.. corresponds to the number of distinct peptides having at least 95% confidence. Multiple modified and cleaved states of the same underlying peptide sequence are considered distinct peptides because they have different molecular formulas. Multiple spectra of the same peptide, due to replicate acquisition or different charge states, only count once. Geomean is the geometric mean of all ratios analysed, corresponding to an average fold change. StouffersPval applies to the combined p-value using Stouffer's method, corresponding to an aggregate measure of significance.

Supplemental Figure S8: Immunoblot images used for densitometry values listed in Figures 1 and Figures 3 and Table 2. Immunoblotting was performed on 10µg protein, following extraction from spermatids purified from TgMsi2 Adult (PND60) (Tg1-3) and Wildtype control (Wt1-3) testes as described in materials and methods (Protein Extraction and Immunoblotting). Relative expression of TBX1 (Figure 1), PIWIL1 (Figure 3) and PCNA, NCL, PIWIL2, MATR3, YBX2, DAZAP1, and TM9SF2 (Table 2) was compared to loading control GAPDH or αTUB. Immunoblots for PCNA and PWIL2 were stripped at re-probed for PIWIL1 and DAZAP1, respectively, prior to loading control. Protein molecular weight is noted in brackets and indicated at appropriate size on blot (→).

Table 1: QPCR validation of top 12 significantly altered transcripts in microarray of TgMsi2 testes. Each gene is listed with full name and symbol, known function, microarray DE value (MA value), and qPCR fold change (FC) (mean ± SE). *p<0.05, **p<0.01, ***p<0.001.

Gene (symbol)	***Role/Function***	***MA Value***	***QPCR FC***
Tissue inhibitor of metalloproteinase 1 (Timp1)	*cell proliferation, anti-apoptosis, early development*	*+4.52***	*+16.41±3.38***
Leucine-rich alpha-2-glycoprotein 1 (Lrg1)	*cell differentiation, signal transduction, cell adhesion, development*	*+4.10***	*+9.44±2.43***
Roundabout, axon guidance receptor, homolog 4 (Drosophila) (Robo4)	*cell migration, proliferation, embryonic development*	*+4.04***	*+1.71±0.06****
Lipocalin 2 (Lcn2)	*iron-trafficking, apoptosis, innate immunity*	*+3.17****	*+4.93±0.92**
Retinol binding protein 1, cellular (Rbp1)	*Retinol transport, reproduction, growth, differentiation*	*+2.79****	*+9.12±3.47**
T-box1 (Tbx1)	***transcriptional regulator, embryo development***	***+1.76****	***+2.66±0.41****
Testicular haploid expressed gene (Theg)	*protein assembly in spermatids*	*-2.1***	*-1.37±0.09**
Growth differentiation factor 9 (Gdf9)	*cell growth, reproductive development*	*-2.34****	*-2.80±0.04****
Homeo box C9 (Hoxc9)	*transcription factor important to morphogenesis*	*-2.44****	*-1.67±0.06**
ADAM metallopeptidase	*membrane-anchored protein,*	*-2.49****	*-2.80±0.03****

domain 30 (Adam30)	*spermatogenesis and fertilization*		
SEC23A (S. cerevisiae) (Sec23A)	*cell morphology/proliferation, ER-Golgi protein trafficking*	*-2.72****	*-3.51±0.02****
Adiponectin, C1Q and collagen domain containing (Adipoq)	*metabolic/hormonal processes, cell growth*	*-3.65***	*-3.17±0.19**

Table 2: Top 20 significantly altered proteins identified via iTRAQ of TgMsi2 spermatids.

Each protein is listed with full name and symbol, summary of function, iTRAQ value and if performed immunoblot densitometry analysis (IB Fold Change), and peptides identified via iTRAQ.

Protein (symbol)	***Role/Function***	***iTRAQ (IB FC)***	***# of independent Peptides***
Musashi homolog 2 (MSI2)	*protein of interest (positive control)*	*7.64 (+2.17)*	*6*
Renalase (RNLS)	*FAD-dependent amine oxidase*	*2.45*	*10*
Phosphatidylethanolamine-binding protein 2 (PBP2)	*spermatogenesis*	*1.74*	*14*
Cystatin-8 (CST8)	*sperm development & maturation*	*1.5*	*4*
Nucleolar RNA helicase 2 (DDX21)	*helicase activity, RNA folding*	*1.42*	*4*
Proliferating cell nuclear antigen (PCNA)	*DNA replication & damage response*	*1.26 (+1.46)*	*7*
Nucleolin (NCL)	*chromatin decondensation, transcription, ribosome assembly,*	*1.23 (+1.31)*	*21*
Piwi-like protein 2 (PIWIL2)	*meiosis, stem cell renewal, piRNA pathway, translation control*	*1.22 (+1.82)*	*20*
Lupus La protein homolog (LA)	*RNA processing, mRNA stabilization*	*1.22*	*8*
Dipeptidase 3 (DPEP3)	*meiosis, testis expressed*	*1.2*	*16*
Matrin-3 (MATR3)	*mRNA stabilization, nuclear retention of defective RNAs*	*-1.2 (-1.1)*	*29*
Y-box-binding protein 2 (YBX2)	*RNA-binding, mRNA storage/translational delay*	*-1.28 (-1.92)*	*23*
Dynein heavy chain 3, axonemal (DNAH3)	*sperm motility - flagella assembly*	*-1.33*	*19*

RNA-binding protein MEX3D (MEX3D)	*RNA binding protein, nucleo-cytoplasmic export*	*-1.34*	*7*
Piwi-like protein 1 (PIWIL1)	*spermatogenesis, piRNA stability, stem cell renewal, RNA silencing, translation*	*-1.35 (-1.13)*	*47*
DAZ-associated protein 1 (DAZAP1)	*RNA-binding, spermatogenesis*	*-1.43 (-1.3)*	*7*
Transmembrane 9 superfamily member 2 (TM9SF2)	*spermatogenesis, protein degradation*	*-1.57 (-1.82)*	*9*
Acrosin-binding protein (ACRBP)	*acrosome reaction*	*-2.22*	*24*
Zona pellucida sperm-binding protein 3 receptor (ZP3R)	*oocyte interactions, spermiogenesis*	*-2.51 (-1.27)*	*10*
Sperm equatorial segment protein 1 (SPESP1)	*spermatogenesis, acrosome development*	*-3.79 (-1.23)*	*6*

Table 3: QPCR of 12 selected significantly altered proteins from TgMsi2 spermatid iTRAQ.

Each gene analysed is listed with gene symbol, full name, qPCR fold change, iTRAQ fold change, and comparison of transcript and protein expression. *p<0.05, **p<0.01, and ***p<0.001.

Gene	***iTRAQ ID Name***	***qPCR***	***iTRAQ***	***Summary***
Msi2	*Musashi RNA-binding protein 2*	*+3.54***	*+7.64****	*increased at transcript & protein level (positive control)*
Pcna	*Proliferating cell nuclear antigen*	*+1.12*	*+1.26****	*increased at protein level only*
Ncl	*Nucleolin*	*+1.78*	*+1.23***	*increased at transcript (NS) & protein level*
Piwil2	*Piwi-like protein 2*	*+1.78***	*+1.22***	*increased at transcript & protein level*
Matr3	*Matrin-3*	*-1.37*	*-1.21****	*decreased at transcript (NS) & protein level*
Ybx2	*Y-box-binding protein 2*	*-1.19*	*-1.28****	*decreased at transcript (NS) & protein level*
Piwil1	***Piwi-like protein 1***	***+1.79****	***-1.35****	***increased transcript & decreased protein expression***

Dazap1	*DAZ-associated protein 1*	*-1.21**	*-1.37***	*decreased at transcript & protein level*
Zp3r	*Zona pellucida sperm-binding protein 3 receptor*	*-5.1*	*-2.51****	*decreased at transcript & protein level*
Spesp1	*Sperm equatorial segment protein 1*	*-1.05*	*-3.85****	*decreased at protein level only*

Figure 1

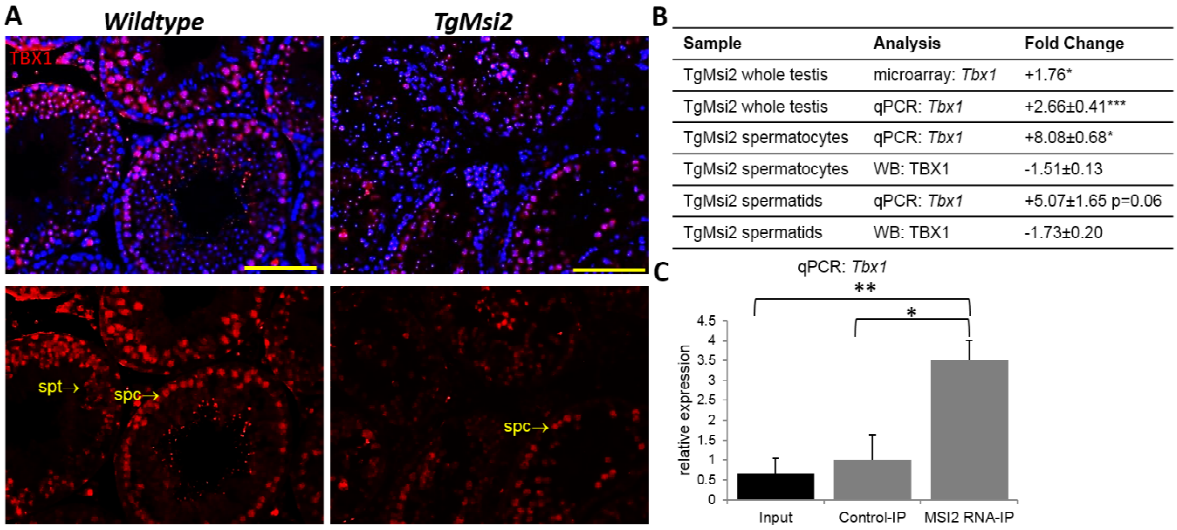

Figure 2

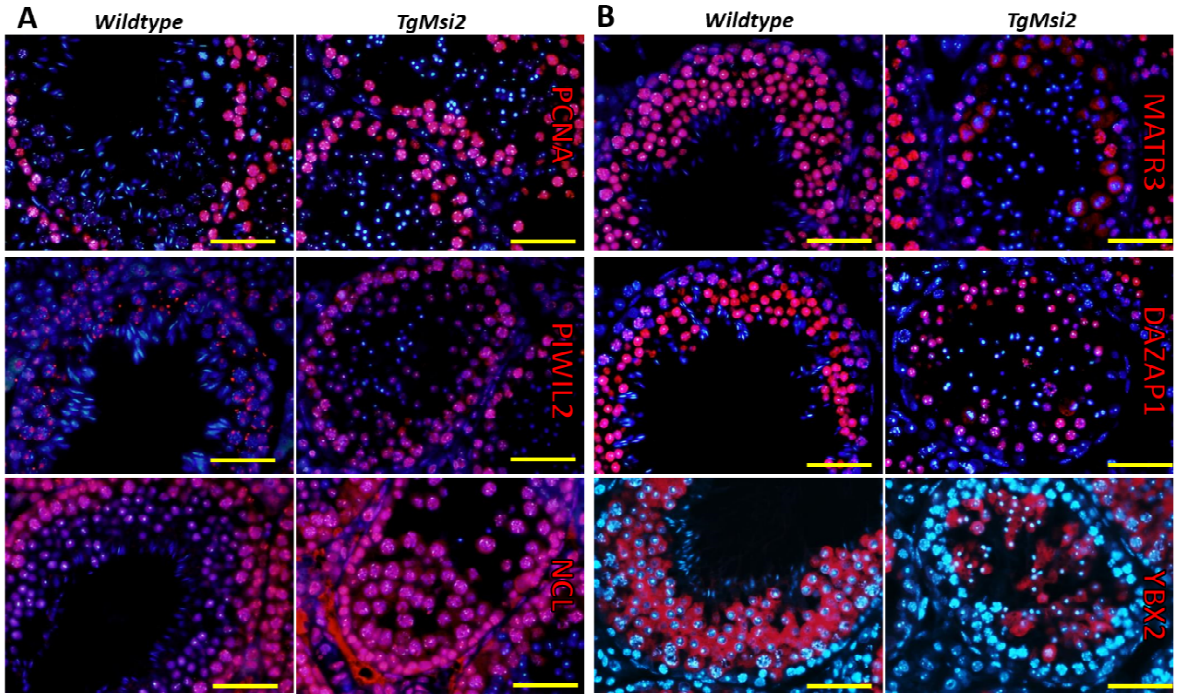

Figure 3

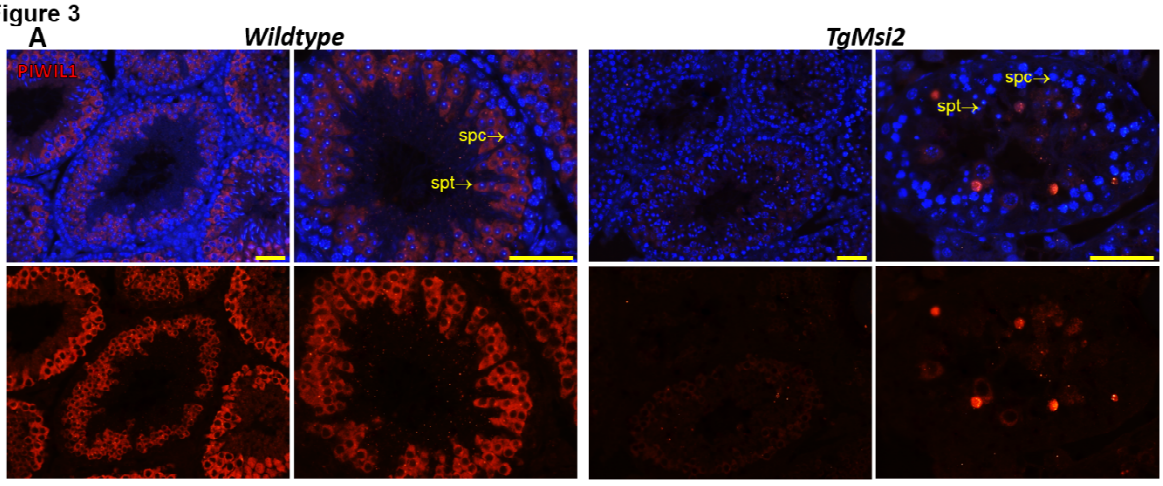

B

Sample	Analysis	Fold Change
TgMsi2 spermatids	iTRAQ: PIWIL1	-1.35***
TgMsi2 spermatids	qPCR: *Piwil1*	+1.79*
TgMsi2 spermatids	WB: PIWIL1	-1.13

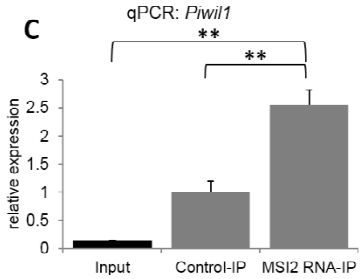

Figure 4

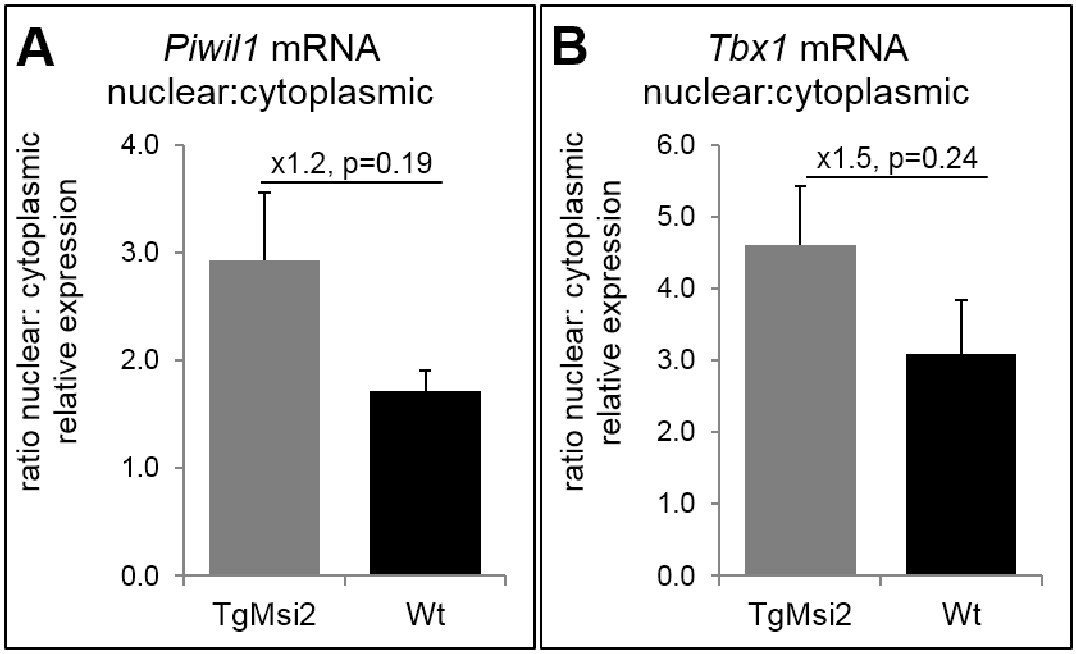

Figure 5

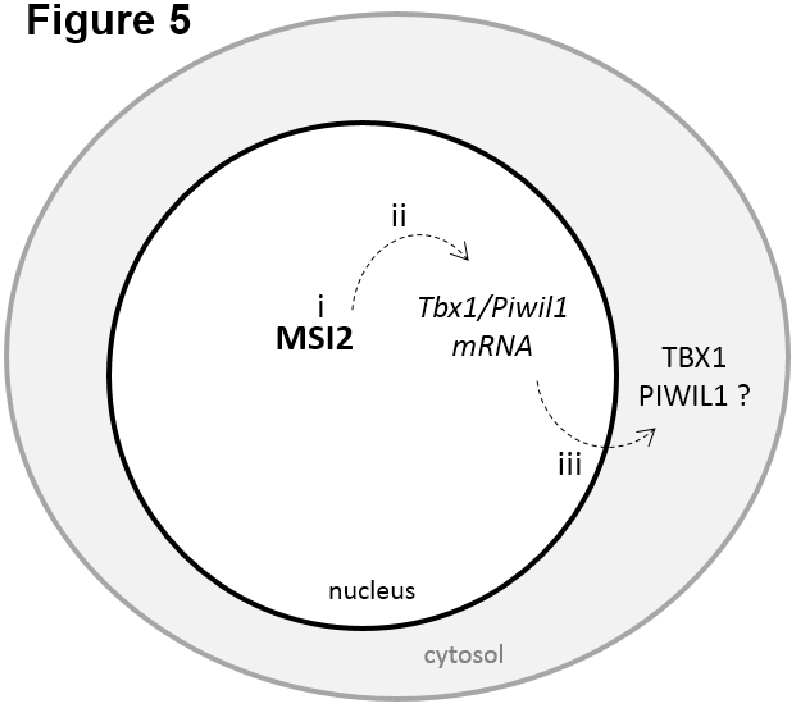

Author/s:
Sutherland, JM; Sobinoff, AP; Fraser, BA; Redgrove, KA; Siddall, NA; Koopman, P; Hime, GR; McLaughlin, EA

Title:
RNA binding protein Musashi-2 regulates PIWIL1 and TBX1 in mouse spermatogenesis

Date:
2018-04-01

Citation:
Sutherland, J. M., Sobinoff, A. P., Fraser, B. A., Redgrove, K. A., Siddall, N. A., Koopman, P., Hime, G. R. & McLaughlin, E. A. (2018). RNA binding protein Musashi-2 regulates PIWIL1 and TBX1 in mouse spermatogenesis. JOURNAL OF CELLULAR PHYSIOLOGY, 233 (4), pp.3262-3273. https://doi.org/10.1002/jcp.26168.